SMALL SCALE MAGNETIC ELEMENTS AS BRIGHT POINTS IN THE BLUE Hα WING

J. Leenaarts[1], P. Sütterlin[1], R. J. Rutten[2], M. Carlsson[3], and H. Uitenbroek[4]

[1]Sterrekundig Instituut, Postbus 80 000, NL–3508 TA Utrecht, The Netherlands
[2]Sterrekundig Instituut, Postbus 80 000, NL–3508 TA Utrecht, The Netherlands; Institute of Theoretical Astrophysics, P.O. Box 1029, Blindern, N–0315 Oslo, Norway
[3]Institute of Theoretical Astrophysics, P.O. Box 1029, Blindern, N–0315 Oslo, Norway
[4]NSO/Sacramento Peak, P.O. Box 62, Sunspot, NM 88349–0062, USA

ABSTRACT

We present a comparison between high resolution observations of the sun at disk center in the blue wing of the Hα line and Hα images synthesized from 3D simulations of magneto-convection. Small scale magnetic elements appear extraordinarily bright in the Hα wing, which is reproduced in the simulation. We show that LTE is a good approximation for Hα wing formation in the photosphere. Small scale magnetic elements appear as bright points because of their low opacity as compared with the surrounding granulation, combined with smaller radial temperature gradient inside the element. We conclude that the wings of Hα are well suited as proxy magnetometer.

1. INTRODUCTION

The Dutch Open Telescope (DOT) was recently equipped with a Lyot filter to observe in the Balmer Hα line. Images taken in the blue wing of the line show local intensity brightenings at the position of the familiar G band bright points which are a valuable proxy for small-scale strong-field magnetic elements in the photosphere (*e.g.,* Muller & Roudier 1984; Berger et al. 2004; Rouppe van der Voort et al. 2005). In this contribution we discuss the formation of the Hα wing in detail using 3D magneto-convection simulations and show that the Hα bright features indeed correspond to kiloGauss field concentrations.

2. OBSERVATIONS

The data analyzed in this paper were acquired using the DOT on October 6, 2004 during the JOP178 campaign concentrating on solar filaments. During excellent seeing conditions a time series (T = 55 min; Δt = 30s) was recorded in five wavelengths (Ca II H, G band, blue and red continuum, Hα with the Lyot filter switching between two positions (line core and -0.08 nm) between consecutive speckle bursts. Figure 1 shows a small cutout from one set of images, showing some network bright points. The G band image shows the familiar brightenings associated with strong magnetic fields, with corresponding emission in the Ca II H and blue Hα wing image. The Hα image shows low granulation contrast, dark streaks at right that are of chromospheric origin and, quite strikingly, bright roundish features that are barely visible or absent in the G band and Ca II H images, for example at $(x, y) = (1, 2)$ and $(0.8, 5)$. Many more can be identified in the full field of view.

3. FORMATION OF THE BLUE WING OF Hα

A number of questions arise from these observations:

- Why are magnetic elements so bright in the Hα wing?
- Why does the Hα wing not show reversed granulation as in the wings of Ca II H&K?
- Why is the granulation contrast so low in the Hα wing?
- How well do Hα-wing bright points map the magnetic field?

We will address these one by one.

3.1. Bright point formation

We use a snapshot from the 3D magneto-convection simulation used by Carlsson et al. (2004) to synthesize G band images. The code is based on Stein & Nordlund (1998). We extracted a 2D slice from this 3D snapshot, with a horizontal extent of 6 Mm and a vertical range

Proceedings of the International Scientific Conference on Chromospheric and Coronal Magnetic Fields, 30 August – 2 September 2005 (ESA SP-596, November 2005)

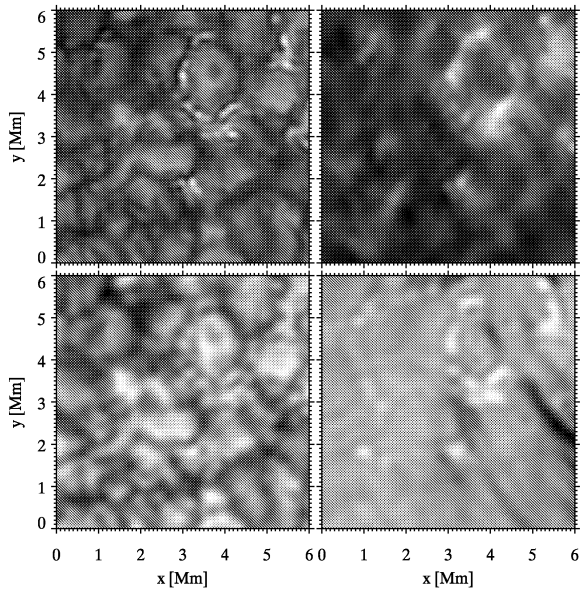

Figure 1. Subfield of observations with the Dutch Open Telescope from October 6, 2004. Upper left: G band. Upper right: Ca II H line center. Lower left: continuum at 650 nm. Lower right: Hα wing at 0.08 nm blue of line center. Small scale magnetic elements are bright in all diagnostics except the continuum. The granulation contrast is exceptionally small in the Hα wing image. Notice the bright point at $(x, y) = (1, 2)$ *which is clearly visible in Hα, but barely shows up in the G band and is absent in the Ca II H image.*

from 0.45 Mm below to 0.5 Mm above the average continuum optical depth unity. On top of this slice we added the FALC chromosphere (Fontenla et al. 1993). We then solved the NLTE radiative transfer equations in PRD for a 4 level hydrogen atom using the RH code of Uitenbroek (2001). The results are shown in Fig. 2.

Panel 5 and 9 show the temperature and the absolute value of the magnetic field strength of the atmosphere. Panel 1 and 3 show NLTE departure coefficients for the $n = 2$ and $n = 3$ levels of hydrogen, the lower and upper level of the Hα line. As can be seen, the lower level population is essentially in LTE throughout the entire photosphere, showing that the opacity closely follows Saha-Boltzmann values. The upper level population is in LTE up to the $\tau = 1$ surface at 656.192 nm. Above $\tau = 1$ the upper level is overpopulated due to overionization in the Balmer continuum, which leads to over-recombination into the $n = 3$ level. This results in $S > B$ in fluxtubes and above granules, as can be seen in panel 7 and 8 (Rutten & Carlsson 1994).

Panel 2 shows the emergent intensity at 656.192 nm, 0.08 nm blue of line center. The LTE intensity is everywhere lower than the NLTE intensity, but only marginally so. The maxima in Hα wing intensity clearly correspond to magnetic field concentrations. Panel 4 shows the contribution function for the NLTE intensity. The small difference between the LTE and NLTE intensity shows that the small deviation from LTE of the source function is unimportant, and together with the LTE behavior of the opacity shows that LTE is a good approximation for Hα wing formation.

Panel 5 and 6 show the temperature on a height scale and an optical depth scale, respectively. The surrounding granulation has a higher temperature at equal geometrical height, but at equal optical depth magnetic elements are hotter, making them appear bright in the Hα wing. This mechanism is basically the same as for the G band (Carlsson et al. 2004; Shelyag et al. 2004).

3.2. Absence of reversed granulation

Observations in the wings of Ca II H&K show reversed granulation, a pattern that looks like granulation in the continuum but with its brightness reversed. This pattern is caused by the reversal of the granular flows, and originates from layers between 0.2 Mm and 0.6 Mm above continuum optical depth unity (Rutten et al. 2004; Leenaarts & Wedemeyer-Böhm 2005).

The lower right panel of Fig. 1 illustrates that reversed granulation is not observed in the Hα wing. The reason is the large excitation energy (10.2 eV) of the lower level ($n = 2$) which makes the line opacity very sensitive to the temperature. Take the simple case of a 2-level atom in LTE. In that case, the relative temperature sensitivity of the upper-level population is $(\mathrm{d}n_2/\mathrm{d}T)/n_2 = \Delta E/kT^2$, where n_2 is the upper-level population and ΔE is its excitation energy.

This sensitivity has a profound effect on the formation of the line, as illustrated in Fig. 3, which compares the formation of Ca II H and Hα in the FALC atmospheric model. The lower-left panel shows the temperature sensitivity of the hydrogen $n = 2$ level, where the relative population drops at the temperature minimum, whereas the lower level of Ca II H, the ground state of the ion, is almost insensitive to the temperature and only responds to the chromospheric temperature rise and density drop where Ca II ionizes to Ca III.

The middle panels show the striking resulting difference in extinction coefficient. Hα has a clear minimum at the temperature minimum, whereas Ca II H shows an almost linear dependence between extinction coefficient and density. In terms of optical depth this is expressed as a plateau in optical depth buildup around $z = 500$ km for Hα.

The emergent intensity I can be expressed as an integral over the contribution function:

$$I = \int_0^\infty S\,\mathrm{e}^{-\tau}\,\mathrm{d}\tau = \int_0^\infty S\,\tau\,\mathrm{e}^{-\tau}\frac{\mathrm{d}\ln\tau}{\mathrm{d}z}\,\mathrm{d}z. \qquad (1)$$

From this decomposition (Carlsson & Stein 1997) it is immediately clear that there is no contribution to the intensity if there is almost no τ buildup at some point in the

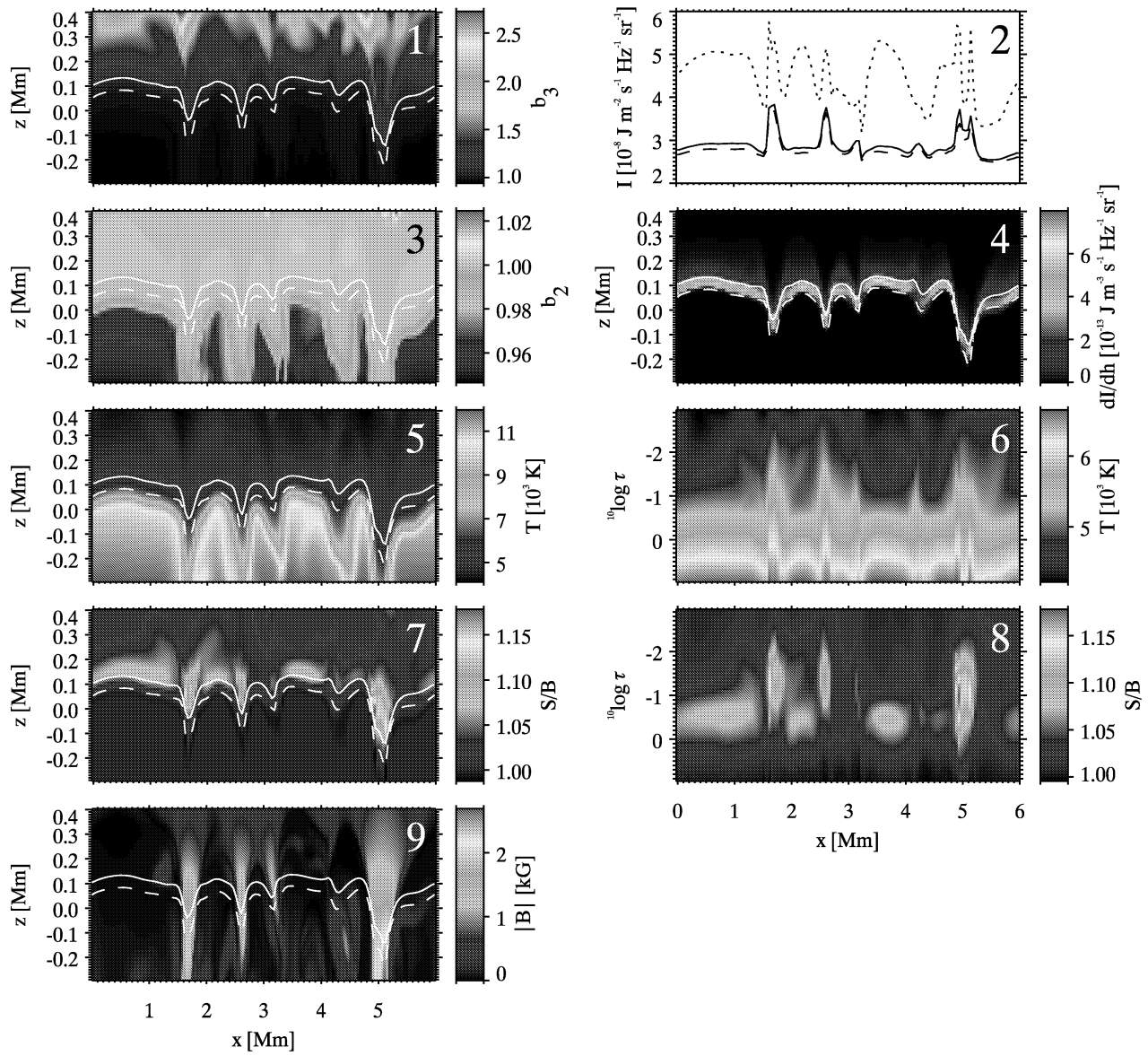

Figure 2. Properties of the 2D atmosphere. The average formation height of the Hα wing at 656.192 nm and the underlying continuum in the (x, z) maps are indicated with solid and dashed lines respectively. The optical depth scales are optical depth at 656.192 nm. 1: departure coefficient of the n = 3 level of the model H atom. 2: emergent intensity at 656.192 nm in NLTE (solid), in LTE (dashed) and the underlying continuum (dotted). 3: departure coefficient of the n = 2 level of the model H atom. 4: contribution function $\mathrm{d}I/\mathrm{d}z$. *5: temperature on a height scale. 6: temperature on an optical depth scale. 7: source function divided by the Planck function on a height scale. 8: source function divided by the Planck function on an optical depth scale. 9: absolute value of the magnetic field strength.*

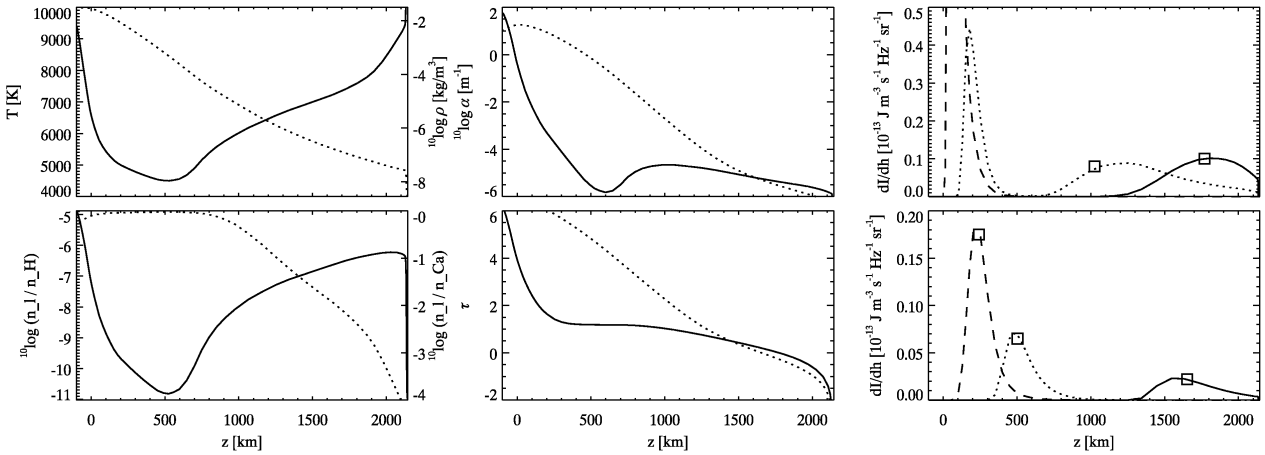

Figure 3. Illustration explaining the difference between Hα and Ca II H wing formation. Upper left: FALC temperature (solid) and density (dotted). Lower left: number density of the lower level of the line relative to the total number density of the atomic species, respectively for Hα (left-hand scale, solid) and for Ca II H (right-hand scale, dotted). Upper middle: line center extinction coefficient for Hα (solid) and Ca II H (dotted). Lower middle: line center optical depth for Hα (solid) and Ca II H (dotted). Upper right: contribution function for different positions in the Hα line. Squares indicate the $\tau = 1$ height. Solid: line center. Dotted: middle wing. Dashed: far wing. Lower right: Same for Ca II H.

atmosphere. This holds for the Hα line around the temperature minimum and is indicated by the double-peaked contribution function in the upper right panel. So even though it is possible to find a wavelength in the line that has $\tau = 1$ at $z = 500$ km, the Eddington-Barbier approximation $I \approx S(\tau = 1)$ does not hold.

3.3. Small granulation contrast

As was shown in the previous subsection, the Hα line extinction coefficient is strongly sensitive to the temperature. Paradoxically, the extinction *sensitivity* makes the emergent intensity *insensitive* to temperature differences as long as the formation is in LTE, with a single peaked contribution function that lies entirely in a part of the atmosphere with an outward decreasing temperature.

As shown in section 3.1 this is the case for the Hα line wing at -0.08 nm from line center. In this case the Eddington-Barbier approximation has better validity and the cartoon in Fig. 4 can be used to explain the small granulation contrast. A temperature difference in the atmosphere as between granules and lanes will give a small contrast.

In addition to this temperature effect, the effect of the granular flow velocities also decrease the contrast. In a lane, the downflow shifts the line out of the wavelength passband, as we are observing in the blue wing. In a granule interior the line is shifted into the passband. Combined with the outward decreasing temperature this results in decreased contrast as well.

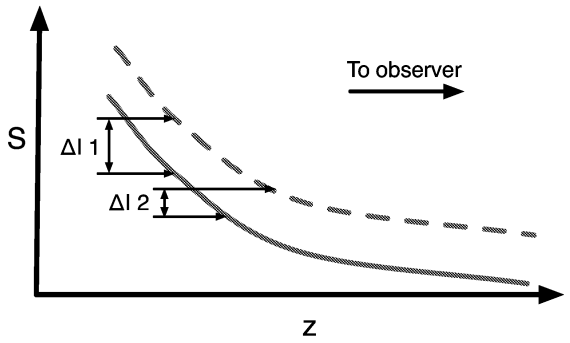

Figure 4. Cartoon explaining the insensitivity of the Hα line wing to temperature variations. The Eddington-Barbier approximation states that the emergent intensity is about equal to the source function S at optical depth unity. For a line that has a temperature-independent opacity (like Ca II H) an increase in atmospheric temperature will not change the $\tau = 1$ height and leads to a significant change in emergent intensity ΔI 1. Hα has a temperature-sensitive opacity. A rise in atmospheric temperature shifts the $\tau = 1$ height to larger values, which together with the outward decreasing temperature results in only a small increase in emergent intensity ΔI 2.

4. 3D SIMULATIONS

The result of section 3.1, that the Hα wings form nearly in LTE, permits us to compute emergent Hα profiles for the full snapshot of the magneto-convection simulation in LTE. We then multiplied these with the DOT filter function of the observations of October 6, 2004. The result

is shown in Fig. 5. The upper-left panel shows the emergent intensity without spatial smearing. The upper-right panel shows the magnetic field strength at continuum optical depth unity. The Hα wing brightness enhancements correspond clearly to magnetic field strength of 1 kG or more.

The lower panels show the simulated intensity for the continuum at 650 nm and in the Hα wing , but smeared with an ideal point-spread function corresponding to the DOT aperture of 45 cm. In addition, the Hα wing image brightness has been scaled to have the same maximum and zero intensity as the observations in Fig. 1. The structures seen in the simulations compare well with the observations. The granulation contrast is small, and the magnetic elements show up as chains of roundish intensity brightenings. The simulated red continuum does also look the same as the observations. The magnetic structures are visible, but are of about equal brightness as the surrounding granules.

It is interesting to compare the simulated Hα wing image with the simulated G band image of Carlsson et al. (2004), computed from nearly the same simulation snapshot. Compared to the G band image, the magnetic elements stand out much clearer in the unsmoothed Hα wing image.

5. CONCLUSIONS

By comparing observations with 3D magneto-convection simulations we have shown that bright points in the blue wing of the Hα line correspond to kiloGauss magnetic field concentrations in the photosphere. These bright points are easily found and tracked due to the small granulation contrast in the images, as compared with for example the G band. In practice the G band or, in the future, the CN bandhead are better suited to study magnetic structures at the smallest observable scales owing to their smaller wavelength (430 nm and 389 nm). But if one is interested in locating and tracking magnetic elements Hα provides a better tool.

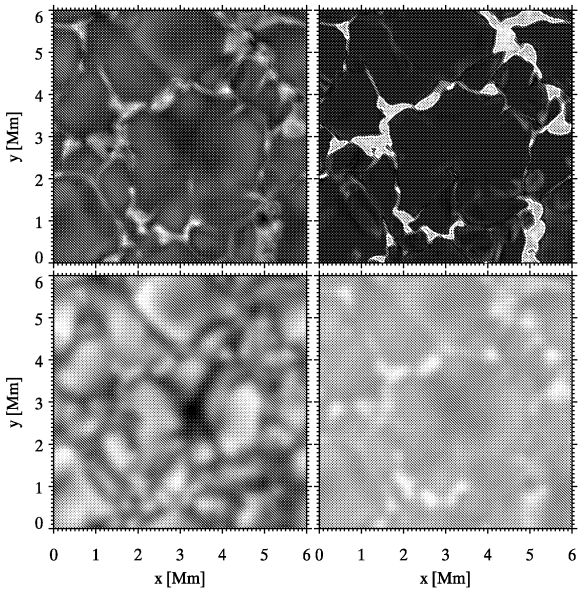

Figure 5. Results from a 3D magneto-convection simulation. Top left: Simulated emergent intensity in the Hα wing. No spatial smearing applied. Top right: magnetic field strength, the grey scale reaches from 0 kG to 2.8 kG. White contour is the 1 kG level. Bottom left: simulated DOT 650 nm continuum image, smeared with an ideal point-spread function corresponding to the DOT aperture of 45 cm. Bottom right: Simulated DOT blue Hα wing image, smeared with an ideal point-spread function. The gray scale has been adjusted to give the same zero and maximum intensity as the Hα panel in the observations of Fig. 1. Notice that the bright features in the Hα image outline regions of kiloGauss field strength.

REFERENCES

Berger, T. E., Rouppe van der Voort, L. H. M., Löfdahl, M. G., et al. 2004, &A, 428, 613

Carlsson, M. & Stein, R. F. 1997, ApJ, 481, 500

Carlsson, M., Stein, R. F., Nordlund, Å., & Scharmer, G. B. 2004, ApJ, 610, L137

Fontenla, J. M., Avrett, E. H., & Loeser, R. 1993, ApJ, 406, 319

Leenaarts, J. & Wedemeyer-Böhm, S. 2005, &A, 431, 687

Muller, R. & Roudier, T. 1984, Sol. Phys., 94, 33

Rouppe van der Voort, L. H. M., Hansteen, V. H., Carlsson, M., et al. 2005, &A, 435, 327

Rutten, R. J. & Carlsson, M. 1994, in IAU Symp. 154: Infrared Solar Physics, 309

Rutten, R. J., de Wijn, A. G., & Sütterlin, P. 2004, &A, 416, 333

Shelyag, S., Schüssler, M., Solanki, S. K., Berdyugina, S. V., & Vögler, A. 2004, &A, 427, 335

Stein, R. F. & Nordlund, A. 1998, ApJ, 499, 914

Uitenbroek, H. 2001, ApJ, 557, 389